PB90-150830

Furnace Sorbent Reactivity Testing for Control of SO2 Emissions from Illinois Coals

(U.S.) Environmental Protection Agency, Research Triangle Park, NC

Dec 89

U.S. Department of Commerce
National Technical Information Service
NTIS

PB90-150830

EPA-600/2-89-065
December 1989

FURNACE SORBENT REACTIVITY TESTING FOR CONTROL OF SO_2 EMISSIONS FROM ILLINOIS COALS

Final Report

Prepared by:

Brian K. Gullett and Frank E. Briden
U.S. Environmental Protection Agency
Air and Energy Engineering Research Laboratory
Research Triangle Park, North Carolina 27711

Prepared for:

Center for Research on Sulfur in Coal
Suite 200, Coal Development Park
Post Office Box 8
Carterville, Illinois 62918-0008

and

U.S. Environmental Protection Agency
Office of Research and Development
Washington, DC 20460

REPRODUCED BY
U.S. DEPARTMENT OF COMMERCE
NATIONAL TECHNICAL INFORMATION SERVICE
SPRINGFIELD, VA. 22161

TECHNICAL REPORT DATA
(Please read Instructions on the reverse before completing)

1. REPORT NO.	2.	3. RECIPIENT'S ACCESSION NO.
EPA-600/2-89-065		
4. TITLE AND SUBTITLE		**5. REPORT DATE**
Furnace Sorbent Reactivity Testing for Control of SO_2 Emissions from Illinois Coals		December 1989
		6. PERFORMING ORGANIZATION CODE
7. AUTHOR(S)		**8. PERFORMING ORGANIZATION REPORT NO.**
Brian K. Gullett and Frank E. Briden		
9. PERFORMING ORGANIZATION NAME AND ADDRESS		**10. PROGRAM ELEMENT NO.**
See Block 12		
		11. CONTRACT/GRANT NO.
		NA (Inhouse)
12. SPONSORING AGENCY NAME AND ADDRESS		**13. TYPE OF REPORT AND PERIOD COVERED**
EPA, Office of Research and Development Air and Energy Engineering Research Laboratory **Research Triangle Park, NC 27711**		Final: 10/88 - 8/89
		14. SPONSORING AGENCY CODE
		EPA/600/13

15. SUPPLEMENTARY NOTES AEERL project officer is Brian K. Gullett, Mail Drop 4, 919/541-1534.

16. ABSTRACT The report gives results of an evaluation of the potential of furnace sorbent injection (FSI) for sulfur dioxide (SO2) emission control on coal-fired boilers burning coals indigenous to Illinois. Tests were run using four coals from the Illinois Basin and six calcium hydroxide--Ca(CH)2--sorbents, including one provided by the Illinois State Geological Survey (ISGS). The evaluation included pilot- and bench-scale sorbent reactivity testing, sorbent microstructure characterization, and injection ash characterization. Pilot-scale FSI testing gave SO2 removal greater than 60%, with some tests (including those with the ISGS sorbent) exceeding 70% removal for Ca/S ratios of 2:1. Bench-scale testing of injection at economizer temperatures (538 C) yielded comparable removals of about 55%. X-Ray diffraction (XRD) tests of the sorbents showed a strong correlation between three measured crystallite microstructural parameters and sorbent reactivity in the FSI tests. Extraction procedure (EP) toxicity tests with the sorbent injection ash gave values well below Resource Conservation and Recovery Act (RCRA) limits for regulated metals.

17. KEY WORDS AND DOCUMENT ANALYSIS

a. DESCRIPTORS	b. IDENTIFIERS/OPEN ENDED TERMS	c. COSATI Field/Group
Pollution	Pollution Control	13B
Coal	Stationary Sources	21D
Combustion		21B
Sulfur Dioxide		07B
Emission		14G
Sorbents		11G
Calcium Hydroxides		

18. DISTRIBUTION STATEMENT	19. SECURITY CLASS *(This Report)*	21. NO. OF PAGES
Release to Public	**Unclassified**	64
	20. SECURITY CLASS *(This page)*	**22. PRICE**
	Unclassified	A04

EPA Form 2220-1 (9-73)

NOTICE

This document has been reviewed in accordance with U.S. Environmental Protection Agency policy and approved for publication. Mention of trade names or commercial products does not constitute endorsement or recommendation for use.

ABSTRACT

Research was undertaken to evaluate the potential of furnace sorbent injection (FSI) for sulfur dioxide (SO_2) emission control on coal fired boilers utilizing coals indigenous to the State of Illinois. Tests were run using four coals from the Illinois Basin and six calcium hydroxide [$Ca(OH)_2$] sorbents, including one provided by the Illinois State Geological Survey (ISGS).

Testing was divided into three tasks:

1. Pilot- and bench-scale sorbent reactivity testing.
2. Sorbent microstructure characterization.
3. Injection ash characterization.

Pilot-scale FSI testing gave SO_2 removal percentages greater than 60, with some tests (including those with the ISGS sorbent) exceeding 70 percent removal for Ca/S ratios of 2:1. Bench-scale testing of injection at economizer temperatures (538 ^{o}C) yielded comparable removals of approximately 55 percent. X-Ray diffraction (XRD) tests of the sorbents showed a strong correlation between three measured crystallite microstructural parameters and sorbent reactivity in the FSI tests. Extraction Procedure (EP) Toxicity Tests with the sorbent injection ash gave values well below Resource Conservation and Recovery Act (RCRA) limits for regulated metals.

TABLE OF CONTENTS

Section		Page
Abstract		ii
List of Figures		iv
List of Tables		v
Acknowledgements		vi
1.0	Executive Summary	1-1
2.0	Introduction and Background	2-1
3.0	Experimental Procedures	3-1
3.1	Innovative Furnace Reactor Tests	3-1
3.2	Graphite Furnace Reactor Tests	3-2
3.3	X-Ray Diffraction Tests	3-5
3.4	Extraction Procedure Toxicity Tests	3-6
3.5	Short Time Differential Reactor Tests	3-6
3.6	Analytical Procedures	3-8
4.0	Results and Discussion	4-1
4.1	Innovative Furnace Reactor Tests	4-1
4.2	Graphite Furnace Reactor Tests	4-6
4.3	Short Time Differential Reactor Tests	4-7
4.4	X-Ray Diffraction Tests	4-9
4.5	Extraction Procedure Toxicity Tests	4-11
5.0	Conclusions and Recommendations	5-1
6.0	References	6-1
Appendix A:	Innovative Furnace Reactor Data	A-1
Appendix B:	Predicting SO_2 Sorbent Reactivity in the Innovative Furnace with X-Ray Diffraction Peak Profiles for the Illinois Center for Research on Sulfur in Coal	B-1
Appendix C:	Quality Control Evaluation Report	C-1

LIST OF FIGURES

Figure		Page
3-1	Innovative Furnace Reactor (IFR)	3-3
3-2	Graphite Furnace Reactor (GFR)	3-4
3-3	Short Time Differential Reactor (STDR)	3-7
4-1	IFR Sorbent Reactivity	4-4
4-2	STDR Alcohol Sorbent Reactivity.	4-8
4-3	Reactivity Predicted by X-ray Line Broadening Versus IFR Data.	4-12
B-1	Reactivity Predicted by XLB Versus IFR	B-15

LIST OF TABLES

Table		Page
4-1	Coal Characteristics	4-2
4-2	Sorbent Characteristics	4-3
4-3	Results from Economizer Injection Tests on GFR	4-6
4-4	Illinois Coal Reactivity and XRD Peak Shape Data	4-10
4-5	Results of EP Toxicity Tests on IFR Ash	4-13
B-1	Illinois Coal Reactivity and XRD Peak Shape Data	B-9
B-2	Derived Regression Functions for Individual XRD Peak Shape Factors	B-11
B-3	Derived Regression Functions for Pairs of XRD Peak Shape Factors	B-13
B-4	Derived Regression Functions for Triplets of XRD Peak Shape Factors	B-14
B-5	Reactivity Prediction from the Two Best XLB Regression Functions Derived from the Observed Reactivities of Coals #1, #6, and #9 Applied to the Individual Coals	B-17
C-1	Data Quality Objectives	C-3

Acknowledgements

The authors wish to acknowledge: the general guidance of Mike Lin and Ken K. Ho of CRSC (Center for Research on Sulfur in Coal), a cofunder of this work under IDENR (Illinois Department of Energy and Natural Resources)/CRSC subgrant agreement 88-142; the technical and editorial support of Kevin R. Bruce and Laura O. Beach of Acurex Corporation, supported by EPA contract 68-02-4701; and the equipment and managerial support of George R. Gillis, U.S. EPA, Air and Energy Engineering Research Laboratory.

1.0 EXECUTIVE SUMMARY

Testing in the Innovative Furnace Reactor (IFR) with four Illinois coals and six sorbents demonstrated sulfur removals in excess of 60 percent at a Ca/S ratio of 2:1. Tests with the lignosulfonate modified Marblehead calcium hydroxide and the Illinois State Geological Survey (ISGS) alcohol calcium hydroxide gave sulfur removals above 70 percent under the same conditions. Removal percentages were lower for the Illinois Basin Coal Sampling Program (IBCSP) #2 coal than for the other coals. This was attributed to its higher pyritic to organic sulfur ratio.

Bench-scale testing of reactivity at economizer temperatures (538 ^{o}C) yielded sulfur removals of roughly 55 percent at a Ca/S of 2:1. Studies were impacted by apparent mass transfer limitations on the rate of reaction.

X-Ray Diffraction tests of the sorbents focused on eight parameters of their crystallite microstructure. Three of these parameters (average column length, modal column length, and strain at maximum column length) were found to correlate strongly with the sorbents' performance in the IFR testing. This may allow a method of predicting sorbent reactivity without costly pilot-scale testing.

Analyses of sorbent injection ash for potential leachability using the Extraction Procedure (EP) Toxicity Tests gave values well below Resource Conservation and Recovery Act (RCRA) limits for all metals tested. While below RCRA limits, the final pH values for these leachates were high enough to elicit concern.

2.0 INTRODUCTION AND BACKGROUND

Emissions of sulfur oxides, principally sulfur dioxide (SO_2), from combustion sources have increased awareness and concern in recent years. In particular, SO_2 emissions from coal-fired boilers used by utilities and industries have been implicated as major contributors to a growing acid precipitation problem. While long-term ecological effects of acid precipitation are being debated, it is clear that a reduction in SO_2 emissions is greatly desirable. Factors to weigh in determining an SO_2 control technology are cost, SO_2 removal efficiency, and ease of retrofitting to existing boilers. The optimum control technology would balance removal levels with the cost to the industry or utility (and ultimately the consumer). One technology that has received considerable attention is Furnace Sorbent Injection (FSI), which offers a relatively low capital cost, ease of retrofitting, and reasonable removal efficiencies.

A large body of research on FSI is currently available. The effects of such fundamental parameters as injection temperature, sorbent type, particle size, and SO_2 concentration have been investigated on the pilot-scale (Beittel et al., 1985; Bortz and Flament, 1985; Snow et al., 1986). These investigations, along with on-going full-scale demonstrations, indicate that SO_2 removals of approximately 60 percent may be expected using commercially available calcium hydroxide [$Ca(OH)_2$] sorbents. Noted potential impacts of FSI on the boiler include increased slagging and fouling, increased mass loading on particulate removal systems, and alteration of the chemical composition of boiler ash.

This current investigation is designed to provide data at the pilot-scale on SO_2 removal from a combustor fired with Illinois Basin coals and injected with a range of sorbent types. These comparative data, along with results from low temperature testing, physical analysis of the sorbents, and chemical analysis of the ash, will be used to evaluate FSI as a control technology for facilities using Illinois Basin coals. Exceptionally high removal efficiencies could expand the range of applications for Illinois high sulfur coal at a lower cost than coal cleaning or wet flue gas desulfurization (FGD) alternatives.

The primary objective of the planned research has been to evaluate FSI as a potential SO_2 emission control technology for coal fired boilers burning Illinois Basin coals. FSI offers the benefits of being less capital intensive than wet FGD as well as the ability to be readily retrofitted to existing facilities with space considerations. To evaluate FSI potential the following specific objectives have been outlined:

1. Develop a data base of sorbent SO_2 removal efficiencies using six sorbents with four coals at two Ca/S ratios in the Environmental Protection Agency's (EPA) Innovative Furnace Reactor (IFR) at a high injection temperature (1,200 ^{o}C) regime.

2. Obtain comparative SO_2 reactivity data for the six sorbents at mid-range temperatures (538 ^{o}C) in EPA's Graphite Furnace Reactor (GFR).

3. Characterize sorbent microstructure properties using x-ray diffraction (XRD) techniques in an effort to correlate these properties with sorbent SO_2 removal efficiencies.

4. Determine the potential for leaching of toxic metals from FSI ash using the EPA's Extraction Procedure (EP) Toxicity Test.

3.0 EXPERIMENTAL PROCEDURES

In the following section, the experimental conditions used in satisfying the objectives outlined in Section 2.0 are given. The four coals used in testing were identified as Illinois Basin Coal Sample Program (IBCSP) #1, #2, #6, and #9. Sorbents chosen for testing included three commercially available calcium hydroxides (Marblehead, Linwood, and Snowflake), a dolomitic hydroxide (Kemidol), a surfactant modified calcium hydroxide (lignosulfonate modified Marblehead), and an alcohol calcium hydroxide provided by the Illinois State Geological Survey (ISGS). The ISGS sorbent was tested by combining equal parts of each of the 10 batches provided. This was necessary to ensure that adequate sorbent was on hand for FSI testing in the IFR. Limited testing of the individual batches was done in the other reactor systems.

3.1 INNOVATIVE FURNACE REACTOR TESTS

Testing in the IFR consisted of determining SO_2 concentrations in the flue gas during sorbent injection while burning each of the coals at feed rates sufficient to yield a firing rate of approximately 49,600 kJ/h (47,000 Btu/h). The SO_2 Continuous Emission Monitor (CEM) was calibrated using multiple calibration gases bracketing measured concentration levels. After establishing a stable baseline SO_2 concentration, sorbent was injected at a Ca/S ratio of approximately 1:1 and the SO_2 level monitored until an equilibrium level was achieved. Sorbent injection was then stopped and the SO_2 level allowed to return to the established baseline prior to repeating the

test. The final SO_2 removal percentage was determined as the average of the duplicate tests. The entire procedure was then reinitiated with a Ca/S ratio of approximately 2:1. The entire test matrix consisted of testing each coal with all six sorbents using duplicate runs (4 coals x 6 sorbents x 2 duplicates x 2 Ca/S ratios = 96 tests). Actual sorbent and coal feed rates were determined gravimetrically. After running on consecutive test days, slagging in the furnace required that it be run overnight with a gas lance in order to deslag the interior prior to reinitiating testing. A diagram of the IFR is shown in Figure 3-1. In all tests the sorbent injection location and temperature were identical to those used in previous comparative tests on the IFR (Snow et al., 1986).

3.2 GRAPHITE FURNACE REACTOR TESTS

Current supply to the electrically heated GFR was regulated to yield a temperature profile with a peak of near 538 ^{o}C (1,000 ^{o}F) while declining rapidly with residence time (or distance) in the reactor. Flow rates sufficient to give a residence time of 0.75 s between 538 and 427 ^{o}C with an SO_2 concentration of 3,000 ppm were used. Each sorbent was injected under differential conditions with respect to SO_2 concentration and conversion to calcium sulfite (or sulfate) determined on solid samples collected by a cyclone separator. Figure 3-2 shows a cross-section of the GFR.

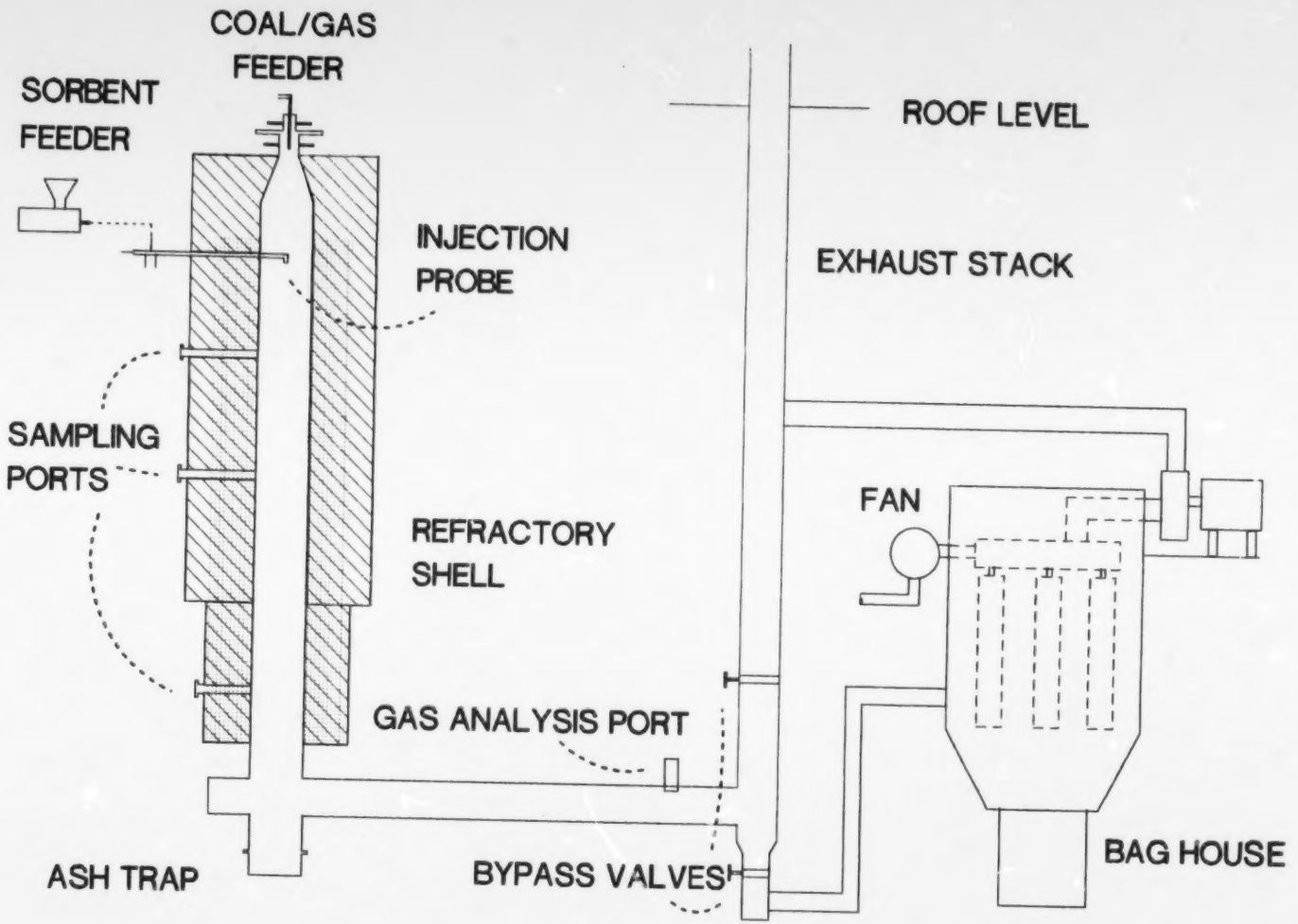

Figure 3-1. Innovative Furnace Reactor.

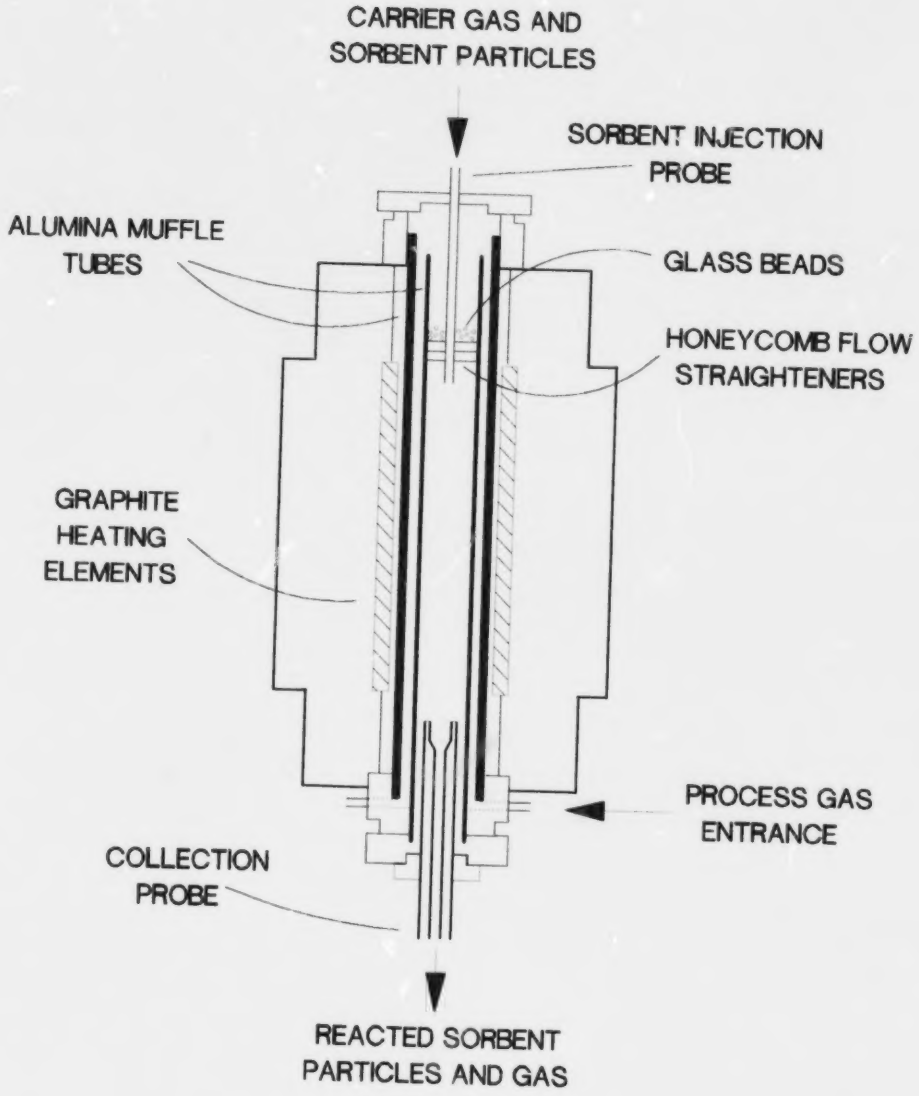

Figure 3-2. Graphite Furnace Reactor.

3.3 X-RAY DIFFRACTION TESTS

Each of the six sorbents was analyzed by XRD using procedures and theory discussed more fully elsewhere (Briden and Natschke, 1988, 1989). The Warren-Averbach method of peak analysis for separation of the crystallite size and strain components was used to determine the following major microstructure properties:

1. Average crystallite size.
2. Frequency of occurrence of column lengths as a function of column length and the column length of maximum frequency of occurrence (modal column length).
3. Half width of the frequency of occurrence of column lengths as a function of column length.
4. Maximum determinable column length.
5. Strain at the average column length.
6. Strain as a function of column length.
7. Strain at the column length of maximum frequency of occurrence.
8. Strain at the maximum determinable column length.

The individual values of the sorbent microstructural properties were related

to IFR-determined reactivities by regression functions to test the hypothesis that various combinations of these properties could predict sorbent reactivity.

3.4 EXTRACTION PROCEDURE TOXICITY TESTS

Toxicity tests were performed on ash taken from the baghouse during each of the baseline coal tests excluding coal #1 for which insufficient sample was collected. Analyses on eight Resource Conservation and Recovery Act (RCRA) regulated metals (antimony, barium, cadmium, chromium, lead, mercury, selenium, and silver) and pH were carried out using methods outlined in EPA method 1310. The tests simulate leachate from a landfill or pond runoff. Ash from sorbent injection using one coal (IBCSP #6) and all six sorbents (Ca/S = 2:1) was also tested to determine the impact of FSI on disposal of ash. Previous work indicated that unreacted calcium oxide (CaO) acts to stabilize most of the metals, but an increase in leachate pH is expected (Dahlin et al., 1986).

3.5 SHORT TIME DIFFERENTIAL REACTOR TESTS

Tests were run on the Short Time Differential Reactor (STDR) using 4 mg of sorbent exposed to process gas consisting of 3,000 ppm SO_2 in 5 percent O_2 and a N_2 balance, preheated to 538 ^{o}C. The reactor, shown in Figure 3-3, is designed to allow fixed bed sample exposure times in the range of 0.3 to 5 s, while maintaining conditions differential with respect to SO_2 concentration.

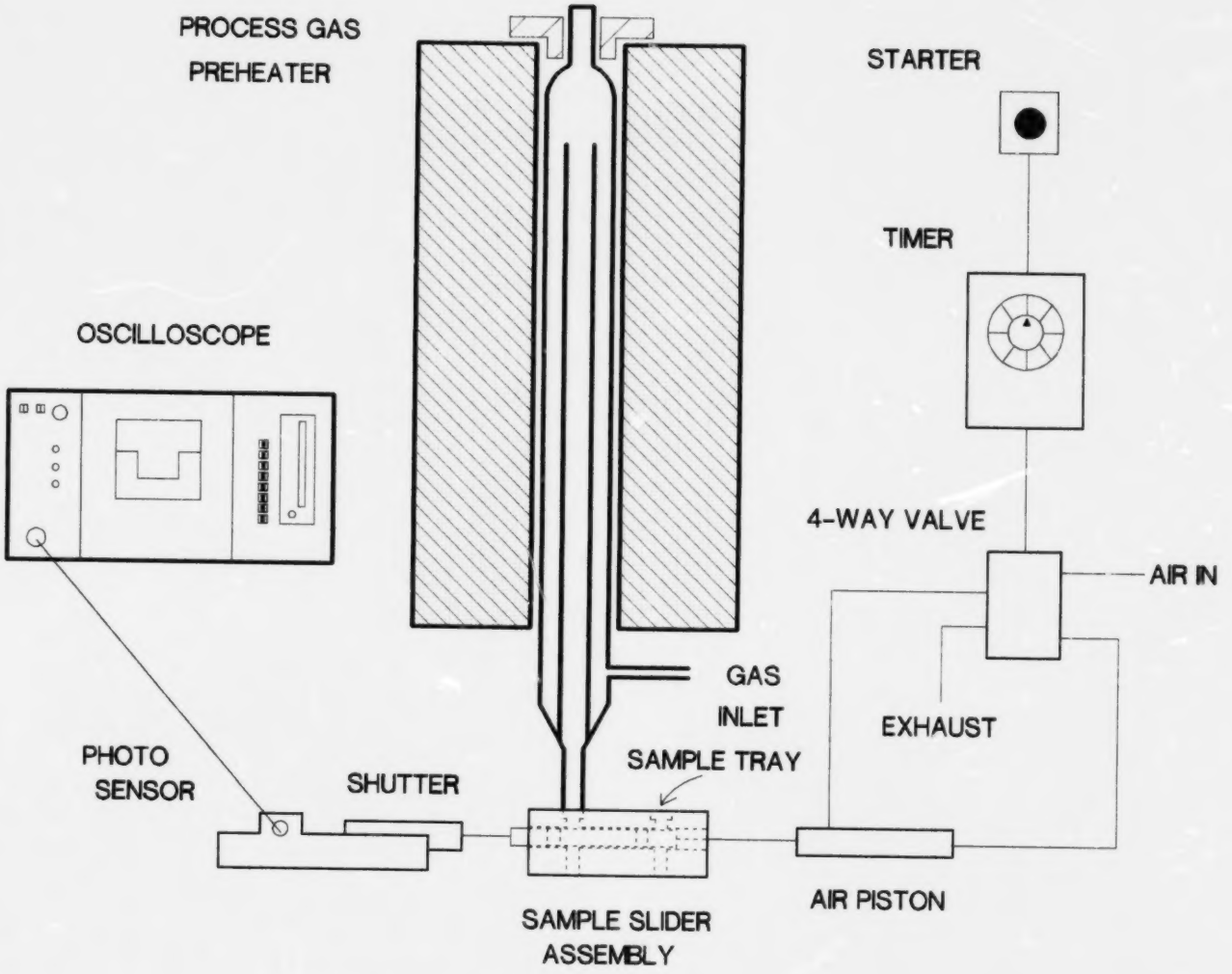

Figure 3-3. Short Time Differential Reactor.

3.6 ANALYTICAL PROCEDURES

Products from the GFR and STDR were analyzed for calcium and sulfate/sulfite concentration by atomic absorption spectroscopy and ion chromatography, respectively. Samples were dissolved in deionized water, 1N HCl, and H_2O_2, and stirred for 5 min. The sample was then filtered into a volumetric flask and diluted for analyses. Sorbent particle size analyses were performed on a Micromeritics Sedigraph 5100. Approximately 0.5 g of sample was dispersed in Micromeritics dispersant A11 and allowed to stir for 15 min. Particle size distributions were determined over the range of 1 to 50 μm in diameter.

4.0 RESULTS AND DISCUSSION

4.1 INNOVATIVE FURNACE REACTOR TESTS

Prior to initiating tests in the IFR, baseline data were collected on the coals and sorbents. Information on the coals, compiled in Table 4-1, was provided by the ISGS. Table 4-2 presents data on the sorbents' physical and chemical characteristics provided by the ISGS and our analyses. Calcium values determined in-house were used in calculating Ca/S ratios in IFR testing.

Results for FSI testing on the IFR are compiled in Figure 4-1. The data presented are estimated SO_2 removal percentages at Ca/S of 2:1, calculated by extrapolating linearly from the mean removals at both Ca/S ratios run for each coal/sorbent combination. Some repeats were necessary due to difficulties encountered in controlling the sorbent feed rate in early tests. The compiled raw data are given in Appendix A.

Figure 4-1 shows several trends in the data. SO_2 capture levels for the IBCSP #2 coal are substantially lower for all sorbents tested (with the possible exception of the Marblehead hydroxide) than for the other coals. It is interesting to note that, while the sulfur content of the IBCSP #2 coal (3.23 percent) is bracketed by the other coals, it differs from them in one important aspect. Unlike the other coals tested, pyritic sulfur accounts for the majority of the sulfur present in IBCSP #2, giving a pyritic/organic

sulfur ratio of 2.53:1 compared to values less than 1:1 for the other coals. No explanation for the apparent adverse effect of a high pyritic/organic sulfur ratio on FSI is currently available. Future work to verify and determine the cause of this phenomenon is needed.

TABLE 4-1. COAL CHARACTERISTICS

	IBCSP #1	IBCSP #2	IBCSP #6	IBCSP #9
Moisture	14.14*	13.62	10.42	6.60
Volatile Matter	44.12	43.34	39.56	35.90
Fixed Carbon	45.62	49.92	51.44	56.10
Ash	10.28	6.66	9.00	8.00
Carbon	67.66	73.31	71.64	74.72
Hydrogen	4.86	5.21	4.73	5.06
Nitrogen	1.18	1.47	1.78	1.77
Oxygen	11.63	10.09	9.05	9.32
Pyritic Sulfur	1.20	2.34	1.83	+
Organic Sulfur	3.00	0.92	1.94	+
Pyritic/Organics Ratio (no units)	0.40	2.53	0.92	+
Total Sulfur	4.26	3.23	3.77	1.17
Calorific Value (kJ/kg)	29,797	31,971	31,314	31,425
Calorific Value (Btu/lb)	12,606	13,526	13,248	13,295

* All values in wt % except where noted.
+ Measurements not taken.

TABLE 4-2. SORBENT CHARACTERISTICS

Sorbent	Ca(wt %)	Median Particle Diameter (μm)
Kemidol	34.3	3.93
Linwood	49.9	2.88
Marblehead	50.1	4.33
Modified Marblehead	50.0	3.47
Snowflake	47.5	3.46
ISGS Mix	47.4	2.06
ISGS BH-16	*	1.90
ISGS BH-20	*	2.67
ISGS BH-22	*	2.24
ISGS BH-24	*	2.01
ISGS BH-29	*	1.68
ISGS BH-30	*	2.09
ISGS BH-31	*	2.01
ISGS BH-32	*	2.35
ISGS BH-33	*	2.08
ISGS BH-34	*	2.41

* Measurements not taken.

Furthermore, when the data from the three other coals (IBCSP #1, #6, and #9) are viewed collectively, the SO_2 removal by individual sorbents does not differ radically from coal to coal. In each case the relative standard deviation of the mean SO_2 removal percentage (standard deviation of mean removal divided by the mean) is less than 10 percent. This could be an indication that the pyritic/organic sulfur ratio of each coal is the largest coal-specific factor in FSI performance using the same sorbent.

The commercially available $Ca(OH)_2$ sorbents (Linwood, Marblehead, and Snowflake) all yield approximately the same values for SO_2 removal percentages when excluding the data from IBCSP #2. The sorbents hydrated under special

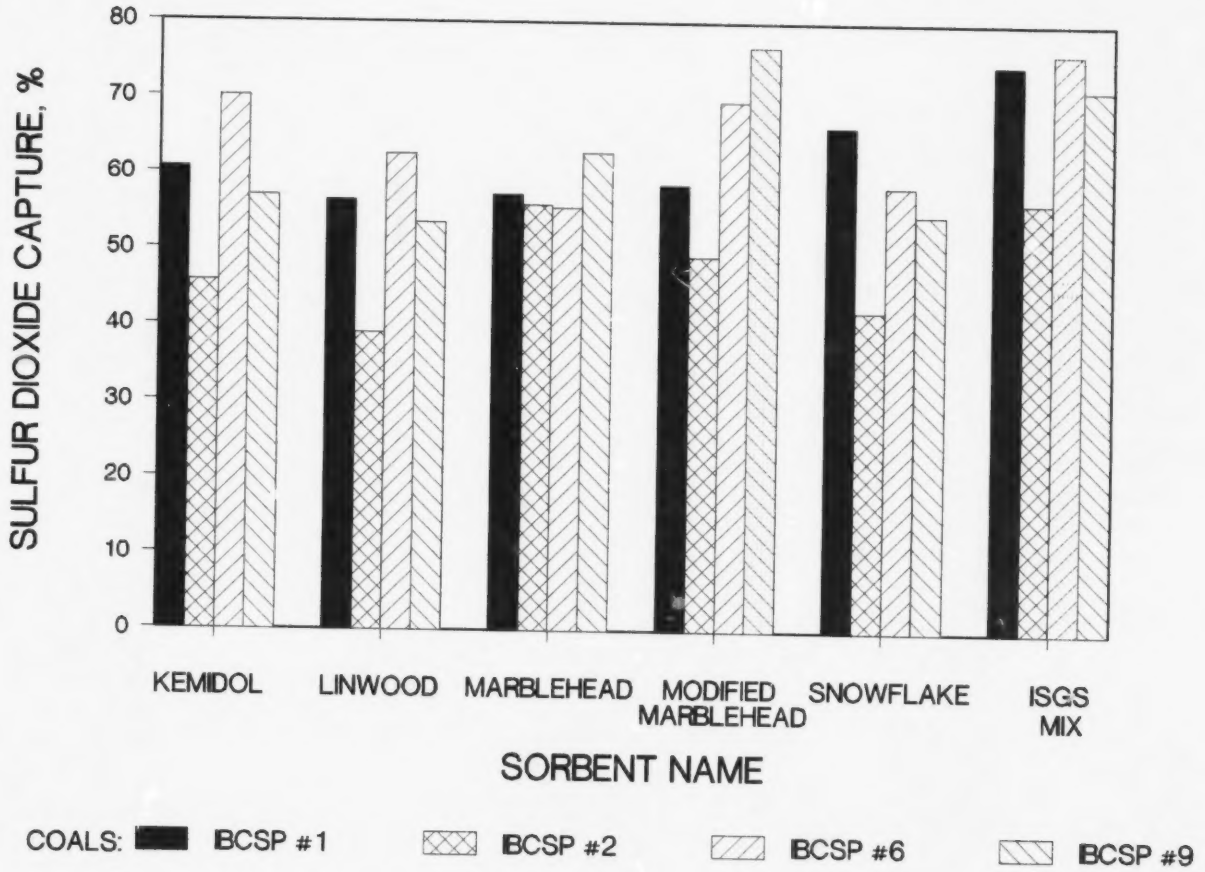

Figure 4-1. IFR Sorbent Reactivity.

conditions (the lignosulfonate modified Marblehead and the ISGS alcohol hydroxide) clearly exhibit superior performance. Past tests (Kirchgessner and Jozewicz, 1988) attribute the enhanced performance of the modified Marblehead to its ability to resist sintering at the high temperatures seen in FSI. The performance of the ISGS sorbent may be related to its very small particle size. Recent EPA in-house tests (Gullett et al., 1988) have demonstrated the importance of sorbent particle size to sulfur capture. Mixing studies have shown that, in many instances, sorbent injection takes place under conditions likely to result in limitations on mass transfer rates of SO_2 to the reacting particle (Newton et al.,1988). In such a regime, ultimate sorbent reactivity will be inversely related to the size of the reacting particle. More work on such mixing phenomena is needed to find ways of injecting sorbent in such a manner as to maximize reaction.

It is interesting to note that for these tests the dolomitic hydroxide, Kemidol, did not outperform the purely calcium-based sorbents. Past tests noted in the literature (Snow et al., 1986) indicate that Kemidol would be expected to yield higher SO_2 removal percentages than the calcitic hydroxides at the same Ca/S ratios. In the tests shown in this work, removal percentages for the dolomitic hydroxide were comparable to those seen for the calcitic hydroxides and were not high enough to offset the increased solids loading on particulate removal systems that necessarily accompanies FSI with dolomitic sorbents due to the unreactive magnesium oxide portion.

The overall impression of the applicability of FSI as an SO_2 control

technology for Illinois coals is positive. With the exception of IBCSP #2, which gave lower results for unknown reasons discussed earlier, SO_2 removals for each of the coal/sorbent tests approached or exceeded 60 percent at a Ca/S ratio of 2:1. Indeed, tests with the specially modified sorbents routinely exceeded 70 percent. These test results strongly recommend FSI as a cost effective means of controlling SO_2 emissions from coal-fired combustors.

4.2 GRAPHITE FURNACE REACTOR TESTS

Results from economizer temperature (538 ^{o}C) sorbent injection testing on the GFR are shown in Table 4-3. The data show a clear inverse relationship to sorbent particle size as measured using the sedigraph; as particle size decreases, the conversion of the sorbent to the calcium sulfite product in the GFR increases. Again, this is indicative of mass transfer resistances acting to control the rate of reaction, rather than other potentially faster

TABLE 4-3. RESULTS FROM ECONOMIZER INJECTION TESTS ON GFR*

Sorbent	Mean Conversion (%)
Marblehead	9.8 ± 0.7
Modified Marblehead	11.0 ± 1.1
Snowflake	11.7 ± 1.0
Linwood	15.2 ± 2.9
ISGS BH-20	17.7 ± 1.0
ISGS BH-24	17.6 ± 1.1
ISGS BH-29	19.9 ± 2.2
Kemidol	15.3 ± 2.5

* Data obtained from minimum of 10 runs at 538 ^{o}C, residence time = 0.75 s, 3,000 ppm SO_2, 5 percent O_2, N_2 balance.

mechanisms such as inherent chemical kinetics. Removing these resistances may show a faster true rate of reaction.

4.3 SHORT TIME DIFFERENTIAL REACTOR TESTS

The STDR is designed to operate under differential conditions with respect to SO_2 concentration. Using small particles, such as in this work, along with a high process gas throughput (resulting in a high gas velocity with respect to the sorbent particles), serves to remove film layer and pore diffusion mass transfer resistances as potential rate limiting steps for the sorbent/SO_2 reaction. Results from testing in the STDR with an SO_2 concentration of 3,000 ppm using ISGS BH-29 sorbent are shown in Figure 4-2. Similar conversions were obtained with Linwood hydroxide over the same time range. These results predict an SO_2 removal of roughly 55 percent for a 1 s residence time and Ca/S ratio of 2:1 when injecting sorbent at or near 538 ^{o}C. This removal percentage is slightly lower than those reported in previous works (Bortz et al., 1986). More work is needed to accurately quantify the fundamental rate of the sorbent/SO_2 reaction under economizer injection conditions using reactors like the STDR prior to predicting potential SO_2 removal levels. The effects of parameters such as SO_2 concentration, sorbent surface area, and sorbent porosity on reaction rate have not been thoroughly investigated.

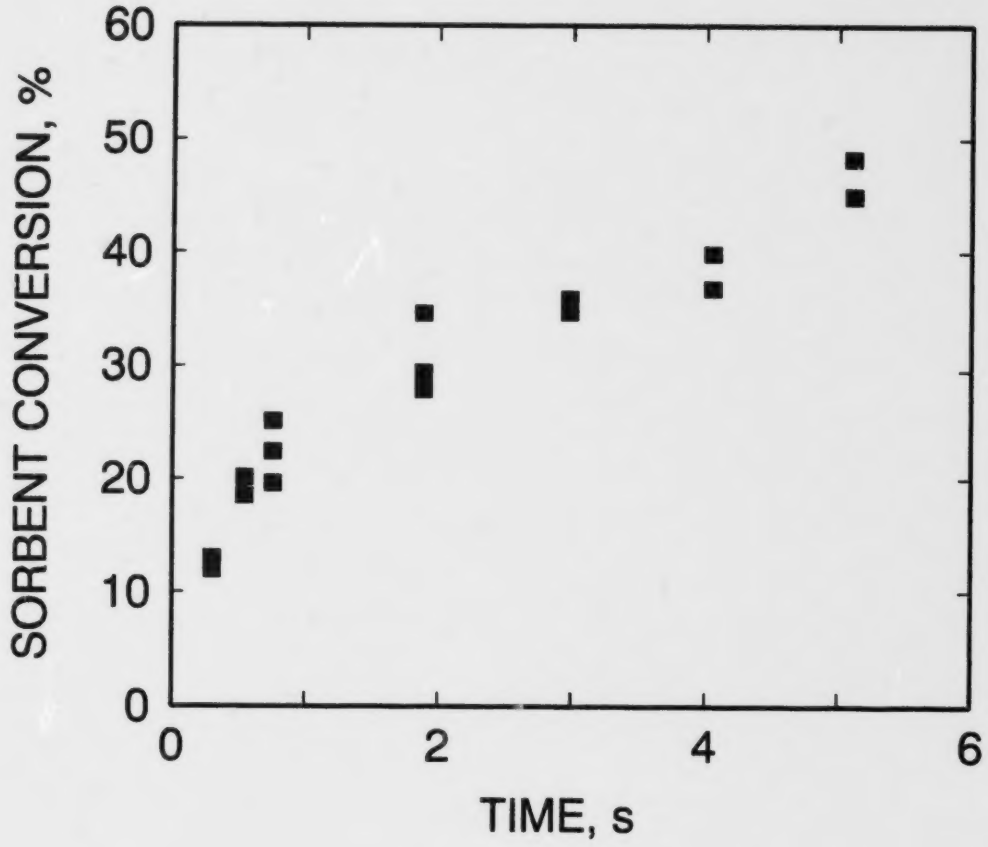

Figure 4-2. STDR Alcohol Sorbent Reactivity

4.4 X-RAY DIFFRACTION TESTS

It has been proposed that crystallite size can affect the gas/solid reactions by modifying the interface between the two phases. It is further proposed that crystal lattice strain could contribute to reactivity by decreasing the stability of the solid and producing a source of activation energy from the strain energy stored in the lattice (Briden and Natschke, 1988). Some of the crystallite size and strain data for the samples analyzed, along with the XRD peak half widths, are shown in Table 4-4. This table gives the percent conversion data from the sorbents tested in the IFR. The percent conversion data are reported in units of moles of Ca reacted divided by moles of Ca available multiplied by 100. The complete XRD results and discussions are contained in Appendix B.

The reactivities for IBCSP coals #1, #6, and #9 were quite similar. The analysis of variance showed a significance level of 0.9 for the sorbents and 0.06 for the coals. Consequently, it was considered reasonable to average the coal reactivities to increase the reliability of the sorbent characterization. To test the hypothesis that the individual x-ray line broadening (XLB) factors were related to reactivities, regression functions were derived using the observed experimental reactivities for coals # 1, # 6, and # 9. For the first stage of this study, it was found that the best single estimator of IFR reactivity was maximum column length, a value representative of the maximum dimension within the distribution of dimensions measured in a crystallite.

Table 4-4. ILLINOIS COAL REACTIVITY AND XRD PEAK SHAPE DATA

	Kemidol	Linwood	Marblehead	Modified Marblehead	Snowflake	ISGS Mix
Reactivity IBCSP #1*	58.7	57.9	57.6	59.8	66.6	76.6
Reactivity IBCSP #2	42.6	38.1	57.3	49.5	47.7	58.8
Reactivity IBCSP #6	67.8	60.1	53.8	67.	57.6	74.2
Reactivity IBCSP #9	52.7	52.3	63.6	75.5	57	69.4
Reactivity Avg #1, #6, #9	59.733	56.766	58.333	67.433	60.4	73.4
Avg Col Lnth**	9.8	11.5	9.9	8.7	15	11.5
Max Col Lnth	45	38	41	32	50	33
Max Freq Col Lnth	3.37	5.33	3.57	3.93	7.47	6.53
Strain (Avg Col Lnth)	2.18 E-3	2.21 E-3	2.2 E-3	2.34 E-3	1.71 E-3	2.22 E-3
Strain (Max Col Lnth)	1.16 E-3	1.34 E-3	1.25 E-3	1.49 E-3	9.1 E-4	1.38 E-3
Strain (Max Frq Col Lnth)	3.27 E-3	2.99 E-3	3.26 E-3	2.84 E-3	2.55 E-3	2.86 E-3

* Reactivities in units of SO_2 removal percentage at Ca/S = 2:1
** Lengths in units of nanometers, nm

In the next stage, regression equations were derived for relating the XLB factors two at a time to the observed IFR reactivities. For the 15 pairs of factors, the correlation coefficients varied from 0.13 to 0.79. The best pair of estimators was maximum column length and the strain at maximum column length with a correlation coefficient of 0.79. This value is considered quite significant, considering its derivation was subject to coal and furnace variability.

Since the increase in correlation was vastly improved by using two factors, the third stage was to use three factors for the analysis. For triplets, the correlation coefficient varied from 0.40 to 0.99. It would appear that it is possible to almost completely characterize the microstructural relation to reactivity with three XLB factors. The best correlation coefficient of 0.99

was derived from the average column length, modal column length, and strain at maximum column length.

Results and predictions obtained from the XLB regression data on the sorbents evaluated can be seen in Figure 4-3. The three XLB factors mentioned above appear to be the best estimators of reactivity from the number of samples analyzed to date. The linear correlation coefficient of 0.99 for the relation is conclusive and is considered reliable for ranking sorbent materials. Future studies of other sorbents could further establish the reliability of this method and its application to ranking sorbent reactivity without undergoing large-scale testing.

4.5 EXTRACTION PROCEDURE TOXICITY TESTS

Results from the EP Toxicity tests are given in Table 4-5. As anticipated, values for all of the regulated metals are below the RCRA limits. Sorbent injection would appear to stabilize many of the metal species, particularly arsenic and cadmium. While the final pH values are below RCRA limits, they are high enough to elicit some concern. Methods for stabilizing the ash or neutralizing leachate from the ash may bear investigation.

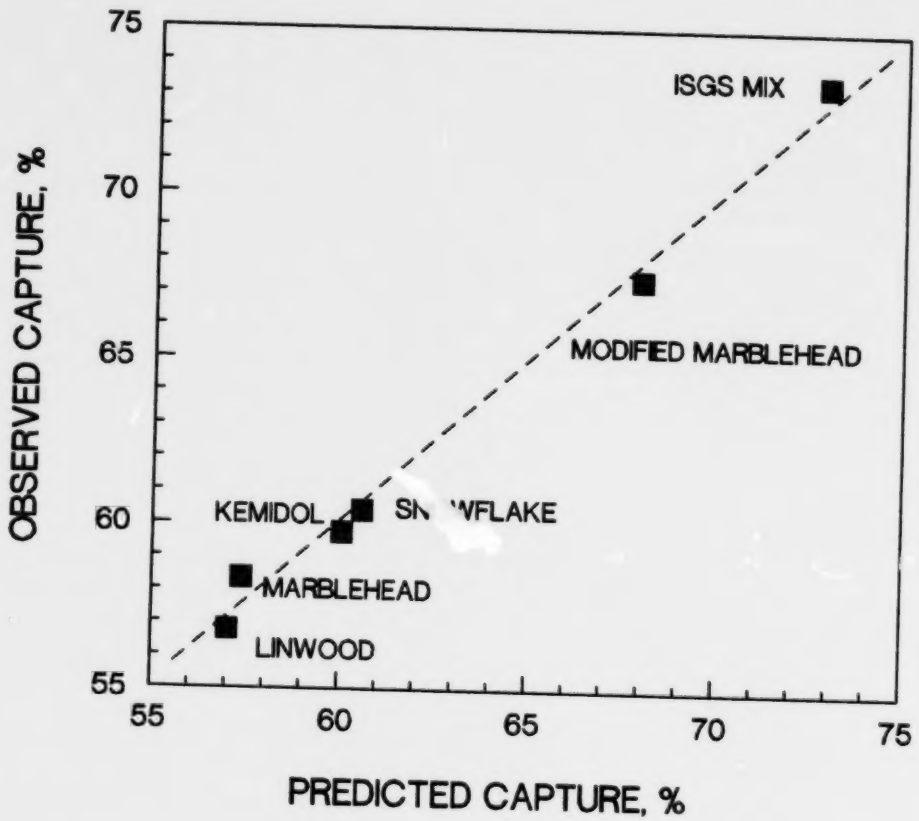

Figure 4-3. Reactivity Predicted by X-ray Line Broadening Versus IFR Data.

TABLE 4-5. RESULTS OF EP TOXICITY TESTS ON IFR ASH

Parameter	EPA Method	RCRA Limit (mg/L)	Coal #2 (mg/L)	Coal #6 (mg/L)	Coal #9 (mg/L)	Kemidol (mg/L)	Linwood (mg/L)	Marblehead (mg/L)	Modified Marblehead (mg/L)	Snowflake (mg/L)	ISGS Mix (mg/L)	Spike Percent Recovery
Arsenic	206.2	5	0.049	0.034	0.069	<0.01	<0.01	<0.01	<0.01	<0.01	<0.01	109
Barium	200.7	100	0.26	0.21	0.26	0.29	0.15	0.12	0.12	0.12	0.093	87
Cadmium	200.7	1	0.11	0.088	0.082	<0.01	<0.01	<0.01	<0.01	<0.01	<0.01	97
Chromium	200.7	5	0.043	0.19	0.36	0.044	0.063	0.072	0.054	0.075	0.071	89
Lead	239.1	5	0.23	0.025	0.13	0.14	0.029	<0.001	<0.001	0.035	<0.001	104
Mercury	245.1	0.2	<0.001	<0.001	<0.001	<0.001	<0.001	<0.001	<0.001	<0.001	<0.001	95
Selenium	270.2	1	<0.01	<0.01	<0.01	<0.01	<0.01	<0.01	<0.01	<0.01	<0.01	71
Silver	200.7	5	0.032	<0.01	0.022	<0.01	<0.01	<0.01	<0.01	<0.01	<0.01	45
Final pH		12.5	5.1	5.0	4.9	12.4	11.9	12.2	11.8	11.9	11.8	NS*

* Not Sampled.

5.0 CONCLUSIONS AND RECOMMENDATIONS

Pilot-scale testing of the SO_2 removal potential of FSI with Illinois Basin coals showed that removals in excess of 60 percent can be readily achieved using commercially available sorbents and a Ca/S ratio of 2:1. The ISGS alcohol sorbent and the marblehead lignosulfonate modified sorbent gave removals in excess of 70 percent. Lower removals were noted for the coal high in pyritic sulfur (as opposed to organic sulfur). Further investigation is necessary to verify and explain this phenomenon. The greatest removals were seen using the ISGS alcohol hydroxide. It is believed that its performance is enhanced by its small particle size and the resultant mixing benefits. More investigation of both bench- and pilot-scale mixing phenomena is necessary to understand how these parameters affect sorbent reactivity. Better injection techniques could minimize particle size effects through greater mixing, yielding increased removals for larger particles.

Testing of sorbent injection at economizer temperatures showed that removals of roughly 55 percent at a Ca/S ratio of 2:1 can be expected. However, not much is currently known about fundamental reaction kinetics for this mid-temperature sorbent/SO_2 reaction. In order to more accurately predict the full-scale performance of injection of sorbent in this temperature region, more work is needed to clarify the effects of temperature, SO_2 concentration, and sorbent characteristics on reactivity.

XRD tests indicated that the sorbent microstructural characteristics of

average column length, modal column length, and strain at maximum column length can provide a basis for prediction of sorbent performance in FSI applications. Verification of the predictive power of these parameters is warranted through testing with additional sorbents.

Analyses of the FSI ash showed that it could be considered nonhazardous in terms of RCRA limits for leaching of heavy metals. The pH of the leachate is a concern, however, because of its alkaline nature. Further investigation into methods of disposal or utilization of FSI waste is necessary.

6.0 REFERENCES

Beittel, R., J.P. Gooch, E.B. Dismukes, and L.J. Muzio. 1985. "Studies of Sorbent Calcination and SO_2–Sorbent Reactions in a Pilot Scale Furnace." Proceedings: First Joint Symposium on Dry SO_2 and Simultaneous SO_2/NO_x Control Technologies, Vol. 1, U.S. Environmental Protection Agency, AEERL, Research Triangle Park, NC, EPA-600/9-85- 020a (NTIS PB85-232353), p.16-1.

Bortz, S., and P. Flament. 1985. "Recent IFRF Fundamental and Pilot Scale Studies on the Direct Sorbent Injection Process." Proceedings: First Joint Symposium on Dry SO_2 and Simultaneous SO_2/NO_x Control Technologies, Vol. 1, U.S. Environmental Protection Agency, AEERL, Research Triangle Park, NC, EPA-600/9-85-020a (NTIS PB85-232353), p. 17-1.

Bortz, S., V.P. Roman, R.J. Yang, and G.R. Often. 1986. "Dry Hydroxide Injection at Economizer Temperatures for Improved SO_2 Control." Proceedings: 1986 Joint Symposium on Dry SO_2 and Simultaneous SO_2/NO_x Control Technologies, Vol. 2, U.S. Environmental Protection Agency, AEERL, Research Triangle Park, NC, EPA-600/9-86-029b (NTIS PB87-120457), p. 31-1.

Briden, F.E., and D.F. Natschke. 1988. "Calcium Hydroxide Sorbent Reactivity with Sulfur Dioxide from X-Ray Diffraction Peak Profiles." Proceedings:

First Combined FGD and Dry SO_2 Control Symposium, Vol. 3, U.S. Environmental Protection Agency, AEERL, Research Triangle Park, NC, EPA-600/9-89-036c (NTIS PB89-172175), p. 7-83.

Briden, F.E., and D.F. Natschke. 1989. "The Characterization of a Solid Sorbent with Crystallite Size and Strain Data from X-ray Diffraction Line Broadening." Accepted for publication in Adv. in X-ray Analysis, 32.

Dahlin, R.S., C.L. Lishawa, and N. Kaplan. 1986. "Analysis of LIMB Waste Management Options." Proceedings: 1986 Joint Symposium on Dry SO_2 and Simultaneous SO_2/NO_x Control Technology, Vol. 2, U.S. Environmental Protection Agency, AEERL, Research Triangle Park, NC, EPA-600/9-86-029b (NTIS PB87-120457), p.39-1.

Gullett, B.K., J.A. Blom, and R.T. Cunningham. 1988. "Porosity, Surface Area, and Particle Size Effects of CaO Reacting with SO_2 at 1100 ^{o}C." React. Solids 6:263.

Kirchgessner, D.A., and W. Jozewicz. 1988. "Laboratory- and Commercial-Scale Results of Testing Surfactant-Modified Sorbent." Proceedings: First Combined FGD and Dry SO_2 Control Symposium, Vol. 2, U.S. Environmental Protection Agency, AEERL, Research Triangle Park, NC, EPA-600/9-89-036b (NTIS PB89-172167), p. 5-121.

Newton, G.H., D.K. Moyeda, G. Kindt, J.M. McCarthy, S.L. Chen, J.A. Cole, and J.C. Kramlich. 1988. Fundamental Studies of Dry Injection of Calcium-Based Sorbents for SO_2 Control in Utility Boilers. U.S. Environmental Protection Agency, AEERL, Research Triangle Park, NC, EPA-600/2-88-069 (NTIS PB89-134142).

Snow, G.C., J.M. Lorrain, and S.L. Rakes. 1986. "Pilot Scale Furnace Evaluation of Hydrated Sorbents for SO_2 Capture." Proceedings: 1986 Joint Symposium on Dry SO_2 and Simultaneous SO_2/NO_x Control Technologies, Vol. 1, U.S. Environmental Protection Agency, AEERL, Research Triangle Park, NC, EPA-600/9-86-029a (NTIS PB87-120465), p.6-1.

APPENDIX A

IFR DATA

IFR DATA

Coal	Sorbent	Baseline SO_2 (ppm)	Injected SO_2 (ppm)	Removal (%)	Ca/S
IBSCP #1	Kemidol	3167	1866	41.1	1.12
	Kemidol	3167	1066	66.3	2.25
	Linwood	3468	2403	30.7	0.87
	Linwood	3468	1703	50.9	1.75
	Marblehead	3180	2302	27.6	0.91
	Marblehead	3180	1504	52.7	1.83
	Mod. Marblehead	3394	2186	35.6	0.93
	Mod. Marblehead	3394	1508	55.6	1.86
	Snowflake	3161	2249	28.8	0.85
	Snowflake	3161	1371	56.6	1.70
	ISGS Mix	3120	1979	36.6	0.79
	ISGS Mix	3120	1204	61.4	1.58
IBSCP #2	Kemidol	2340	1632	30.2	1.12
	Kemidol	2340	1170	50.0	2.24
	Linwood	2469	1852	25.0	0.94
	Linwood	2469	1536	37.8	1.91
	Marblehead	2433	1560	35.9	0.92
	Marblehead	2433	1139	53.2	1.85
	Mod. Marblehead	2332	1765	24.3	0.91
	Mod. Marblehead	2332	1271	45.1	1.82
	Snowflake	2541	1890	25.6	0.88
	Snowflake	2541	1472	42.1	1.75
	ISGS Mix	2288	1538	32.8	0.85
	ISGS Mix	2288	1136	50.3	1.70
IBSCP #6	Kemidol	2817	1488	47.2	1.12
	Kemidol	2817	659	76.6	2.25
	Linwood	2746	1546	43.7	1.15
	Linwood	2746	842	69.3	2.30
	Marblehead	2722	1517	44.3	1.03
	Marblehead	2722	1187	56.4	2.07
	Mod. Marblehead	2788	1436	48.5	1.11
	Mod. Marblehead	2788	702	74.8	2.22
	Snowflake	2918	1852	36.5	1.10
	Snowflake	2918	1058	63.7	2.21
	ISGS Mix	2862	1151	59.8	1.07
	ISGS Mix	2862	610	78.7	2.14
IBSCP #9	Kemidol	882	498	43.5	1.33
	Kemidol	882	260	70.5	2.66
	Linwood	1075	766	28.7	1.06
	Linwood	1075	464	56.8	2.12
	Marblehead	908	624	31.2	0.87
	Marblehead	908	404	55.5	1.74
	Mod. Marblehead	869	533	38.7	1.08
	Mod. Marblehead	869	144	83.4	2.16
	Snowflake	1032	611	40.8	0.92
	Snowflake	1032	488	52.7	1.84
	ISGS Mix	960	508	47.1	1.16
	ISGS Mix	960	186	80.6	2.32

APPENDIX B

PREDICTING SO_2 SORBENT REACTIVITY IN THE INNOVATIVE FURNACE WITH X-RAY DIFFRACTION PEAK PROFILES FOR THE ILLINOIS CENTER FOR RESEARCH ON SULFUR IN COAL

PREDICTING SO_2 SORBENT REACTIVITY IN THE INNOVATIVE FURNACE WITH X-RAY DIFFRACTION PEAK PROFILES FOR THE ILLINOIS CENTER FOR RESEARCH ON SULFUR IN COAL

INTRODUCTION

It was observed early in the history of x-ray diffraction (XRD) analysis that the spectral peaks were not discrete lines as the Bragg equation would predict for a perfect crystal lattice. Instead, the intensities decrease gradually from the maximum at the Bragg angle. XRD line broadening (XLB) comes about from decreasing crystallite (grain size), increasing crystal lattice distortion, and instrument effects.

It is apparent that crystallite size can affect gas/solid reactions by modifying the interface between the two phases. It has been further proposed that crystal lattice strain could contribute to reactivity by decreasing the stability of the solid and providing a source of activation energy from the strain energy stored in the lattice. The first attempt to relate sorbent conversion to crystallite microstructure factors was reported by Briden and Natschke (1).

THEORY

X-ray powder diffraction (XRD) is today, the most powerful technique available for the identification of chemical compounds or phases present in

solid materials. XRD is possible because of the geometric order of solids. The degree of order can vary from almost nothing, as in glasses, to very high order in materials such as quartz. Even such amorphous materials as glass, rubber, and petroleum jelly do exhibit some order which is manifested as XRD spectra with a few very broad peaks. Most solids show sufficient XRD spectra to enable their identification by comparison to standard recorded spectral files. Unknowns consisting of pure phases or mixtures can be identified by executing systematic searches against a standard data base by manual methods or with computer assistance. As a general rule, the limits of detection for individual components of a mixture are about 5 percent.

The XRD spectra, as mentioned earlier, arise from the order within a solid material. From the angle of reflection, θ, of an x-ray beam, with wavelength λ (1.54056 Å for copper Kα1 radiation), one can determine the spacing between the planes, d, from the Bragg equation, which states that the sine of the angle of diffraction is equal to the reflection order times the wavelength divided by two times the d spacing.

If a crystalline material were perfect and every respective distance, d, for each family of planes in the material were precisely repeated (and if the x-ray measuring device were perfect), all of the x-ray intensity would, for each given d space, be reflected only at the respective Bragg angle θ. However, no crystalline material is perfect (true also for x-ray measuring devices); consequently, the reflected x-ray intensity for the d value does not all occur as an infinitesimally narrow line but is distributed in a pattern

with maximum intensity at the Bragg angle and decreasing in both directions going away from the Bragg angle.

Crystalline materials can be imperfect in a number of ways. Most solid materials are not one single contiguous crystal lattice, but are composed of agglomerations of many small crystallites. The crystallite is the largest uninterrupted crystal unit. When crystallites are smaller than 1000 Å, the width of diffraction peaks starts to increase. This enables a measurement of crystallite dimensions down to a limit where they approach the dimensions of the x-ray radiation.

Another type of imperfection which can occur in a crystal is distortion. Distortion is caused by significant variations in the d spacing. This can happen when an alien species is introduced into the crystal lattice; e.g., potassium impurity in sodium chloride. It can also come about from other than ideal crystallization conditions such as rapid temperature change or the presence of surface active agents. Other types of distortion can occur from slippage of crystal planes which takes place during cold working of ductile materials, such as metals.

It has been described how the profile of the XRD peak is affected by three factors: the instrument effects, the crystallite size, and the distortion within the crystal lattice. The first attempt to relate peak shape to crystallite size was by Scherrer (2), who derived the following expression for the peak half width B, in radians, as a function of the radiation

wavelength, the crystallite dimension L, in Å, and the Bragg angle:

$$B\ (2\theta) = 0.94/L \cos \theta$$

It has been postulated that peak broadening due to small crystallite size is of the Cauchy or Lorentzian form while peak broadening due to lattice distortion is of the Gaussian form. Several techniques for separation of size and strain effects attempt to utilize this property (Schoening, 3). These methods have an advantage in needing XRD data for only one peak but are limited in the amount of information given and theoretical rigor.

The most powerful method for separation of size and strain effects available, at present, is that originally proposed by Warren and Averbach (4), Warren (5), and Klug and Alexander (6). According to Warren, the distribution of diffracted power can be expressed as a Fourier series. If only symmetrical contributions to peak broadening are considered, then only two cosine terms of the peak profile function need to be considered. One cosine coefficient is independent of XRD peak order and is related to crystallite column length while the other coefficient is dependent on XRD peak order and is related to crystallite strain. Before the size and strain effects can be separated the instrument effects must be removed. To do this it is first necessary to remove the asymmetry of the experimental XRD peak which is caused by the $K\alpha 2$ peak contribution to the larger $K\alpha 1$ peak. Fourier coefficients are then derived to fit the corrected experimental data. The instrument effects on line broadening can be removed by dividing the Fourier coefficients of the

sample XRD peak by those of a standard material which has relatively minimal line broadening from size or strain. Finally, a set of Fourier coefficients are available which contain only size and strain effects.

The Warren-Averbach method for separating the size and strain components entails the determination of Fourier coefficients to fit the diffraction peaks. This calculation was highly complicated before the development of modern computers. Today the necessary calculations take relatively little time. The Kα2 interference is then corrected and the instrument effects are removed. Finally the size and strain effects are separated through development of equations where the strain is derived from the slope of the expression while the size comes from the Y intercept. From these data come the frequency of occurrence of column lengths and mean squared strains as a function of column length.

EXPERIMENTAL

Six samples of sorbent were evaluated with four different coals in the innovative furnace reactor operating as described earlier.

The experimental data were taken on a Siemens D-500 diffractometer. A copper x-ray tube was used running at 50 kV and 40 mA. A 1 degree entrance aperture and 0.05 degree receiving slit were used. A scintillation detector equipped with a graphite monochrometer was used. The sample powders were packed in a side loading cell. The diffractometer was run and the data were

processed with the Siemens DIF 500, version 1.1 operating system.

At the beginning of the study, a complete XRD scan was taken on a sample of the sorbent material. The phase was identified as JCPDS No. 4-733. Because of the relative high intensities and their isolation, the first (101) and second (202) order peaks seen at the two-θ angles of 34.1 and 76.8 degrees were chosen for the first Warren-Averbach analysis. Zinc oxide (JCPDS No. 36-1451) was chosen as the standard, to account for instrument line broadening, because it had peaks close by (36.26 and 76.77 degrees) which were very narrow. Before running the Warren-Averbach analysis, the experimental XRD peak data were fitted to one of several available functions. The adoption of this step has been an extremely important advance in peak analysis because it smooths out random noise and removes smaller interfering peaks. Without very smooth data it is not possible to get meaningful results, according to Zorn (7) and Langford and Delhez (8). The split Pearson VII function was used for our data, allowing flexibility in fitting complex peaks ranging from pure Gaussian to pure Lorentzian.

RESULTS AND DISCUSSION

The Warren-Averbach analysis provides much information about the microstructure. The major properties delineated are:

1. Average crystallite size.

2. Frequency of occurrence of column lengths as a function of column length, and the column length of maximum frequency of occurrence (or modal column length).

3. Half width of the frequency of occurrence of column lengths as a function of column length.

4. Maximum determinable column length.

5. Strain at the average column length.

6. Strain as a function of column length.

7. Strain at the column length of maximum frequency of occurrence.

8. Strain at the column length of maximum determinable column length.

Some of the crystallite size and strain data, along with the XRD peak half widths, are shown in Table B-1. This table gives the percent conversion data from the reactions of six $Ca(OH)_2$ sorbent samples with four coals plus the average of three coals. It was seen that the reactivities for coals 1, 6, and 9 were quite similar. The analysis of variance showed a significance level of 0.9 for the sorbents and 0.06 for the coals. Consequently, it was considered reasonable to average the coal reactivities to increase the reliability of the sorbent characterization to test the hypothesis that the

TABLE B-1. ILLINOIS COAL REACTIVITY AND XRD PEAK SHAPE DATA

	Kenidol	Linwood	Marblehead	Modified Marblehead	Snowflak	ISGS
Reactivity IBCSP 1 +	58.7	57.9	57.6	59.8	66.6	76.6
Reactivity IBCSP 2 +	42.6	38.1	57.3	49.5	47.7	58.8
Reactivity IBCSP 6 +	67.8	60.1	53.8	67	57.6	74.2
Reactivity IBCSP 9 +	52.7	52.3	63.6	75.5	57	69.4
Reactivity Avg 1,6,9 +	59.733	56.766	58.333	67.433	60.4	73.4
Avg Col Lnth*	9.8	11.5	9.9	8.7	15	11.5
Max Col Lnth*	45	38	41	32	50	33
Max Freq Col Lnth*	3.37	5.33	3.57	3.93	7.47	6.53
Strain (Avg Col Lnth)	2.18E^{-3}	2.21E^{-3}	2.22E^{-3}	2.34E^{-3}	1.71E^{-3}	2.22E^{-3}
Strain (Max Col Lnth)	1.16E^{-3}	1.34E^{-3}	1.25E^{-3}	1.49E^{-3}	9.1E^{-4}	1.38E^{-3}
Strain (Max Freq Col Lnth)	3.27E^{-3}	2.99E^{-3}	3.26E^{-3}	2.84E^{-3}	2.55^{-3}	2.86E^{-3}

+ Reactivity in percent, %

* Lengths (Lnth) in units of nanometers, nm

individual XLB factors were related to the reactivities. Regression functions were then derived to convert each of the factors to reactivity, using the observed experimental reactivities for coals 1, 6, and 9. The percent conversion data are reported in units of moles of Ca reacted divided by moles of calcium available times 100.

In a previous study, it had been found that each of the factors listed above was related to reactivity (Briden and Natschke, 1). In that study, the same starting materials were used, and they varied only by the concentration of an additive. Conditions were more precisely controlled in a flow reactor with SO_2 supplied in a gaseous stream to sorbent material suspended on quartz wool. In the current study, involving a number of quite dissimilar sorbents, the same simple factors were not sufficient to predict reactivity. The linear correlation coefficients (LCC) for each factor are shown in Table B-2. The regression function used was $Y = AX + B$ where Y was observed reactivities, A was the regression coefficient, X was the XLB factor, and B was the regression equation constant. From the table it is seen that the best estimator of reactivity was maximum column length with an LCC of only 0.41. Under some conditions, with some types of data, some investigators might consider an LCC of 0.41 as having some significance, but a higher LCC was desired, in this case, to accept the possibility of a relationship.

For the data reported on in the previous study (Briden and Natschke, 1) the LCCs were computed after publication. The LCCs varied from about 0.62 to 0.94 for single factors. However, when pairs of factors were used in the

TABLE B-2. DERIVED REGRESSION FUNCTIONS FOR INDIVIDUAL XRD PEAK SHAPE FACTORS

	Linear Correlation Coefficient	Regression Function Coefficient	Regression Function Constant
Average Column Length*	0.02	-0.38	66.9
Maximum Column Length*	0.41	-0.589	86.2
Modal Column Length*	0.07	1.03	57.5
Strain at Avg. Column Length	0.07	7830.	45.9
Strain at Max. Column Length	0.22	14800.	44.2
Strain at Mod. Column Length	0.12	-8130.	86.9

* Lengths in units of nanometers, nm

regression, LCCs ranging from 0.721 to 0.993 were observed. When triplets of factors were used, the LCCs ranged from 0.94 to 0.993. Since the use of more factors offered better correlation, presumably because of the consideration of more microstructure factors, it was obvious that the same might help for the current study.

In the next step, regression equations were derived for relating the XLB factors, two at a time, to the observed reactivities. For the 15 pairs of factors, the LCCs varied from 0.13 to 0.79. The regression equation used was $Y = AX_1 + BX_2 + C$ where again Y was observed reactivities, A and B were the respective coefficients for the factors, X_1 and X_2 were the XLB factors, and C was the equation constant. The results are shown in Table B-3. The next best pair of estimators was average column length and modal column length, with an LCC of 0.78. These values were considered quite significant, considering their derivation was subject to variation in the coal and furnace variability. Since the increase in correlation was vastly improved by using two factors instead of one, it was natural to go on to three factors for the analysis. The results are given in Table B-4. For triplets of factors, the LCCs varied from 0.40 to 0.99. It would appear that it is possible to almost completely characterize the microstructure contribution to reactivity with three XLB factors. The best LCC of 0.99 came from the parameters average column length, modal column length, and strain at maximum column length. A plot showing the regression of these data and the observed reactivity data is given in Figure B-1.

TABLE B-3. DERIVED REGRESSION FUNCTIONS FOR PAIRS OF XRD PEAK SHAPE FACTORS

Function Variable Coefficients							
Average Column Length*	Maximum Column Length*	Modal Column Length*	Strain at Average Column Length	Strain at Maximum Column Length	Strain at Modal Column Length	Function Constant	Linear Correlation Coefficient
1.19	-0.89	--	--	--	--	82.1	0.52
-5.49	--	7.43	--	--	--	86.1	0.78
2.18	--	--	27900	--	--	-21.3	0.16
1.50	--	--	--	27100	--	12.0	0.33
-2.08	--	--	--	--	-19700	144.0	0.39
--	0.67	1.6	--	--	--	81.3	0.58
--	1.18	--	-22700	--	--	158.0	0.61
--	-2.82	--	--	-78900	--	274.0	0.79
--	-0.614	--	--	--	- 9220	114.0	0.57
--	--	3.41	26200	--	--	-10.6	0.49
--	--	2.14	--	22270	--	23.9	0.48
--	--	-0.303	--	--	- 9740	93.1	0.13
--	--	--	-32000	46900	--	72.5	0.40
--	--	--	21800	--	-18700	71.2	0.49
--	--	--	--	18900	- 1180	73.8	0.46

* Lengths in units of nanometers, nm

TABLE B-4. DERIVED REGRESSION FUNCTIONS FOR TRIPLETS OF XRD PEAK SHAPE FACTORS

Function Variable Coefficients							
Average Column Length*	Maximum Column Length*	Modal Column Length*	Strain at Average Column Length	Strain at Maximum Column Length	Strain at Modal Column Length	Function Constant	Linear Correlation Coefficient
-16.3	1.6	18.6	--	--	--	85.1	0.96
- 2.27	-1.5	--	-51900	--	--	259.	0.67
- 2.56	-4.45	--	--	-154000	--	462.	0.93
0.0117	-0.616	--	--	--	- 9164	114.	0.57
-10.7	--	10.3	-35160	--	--	205.	0.90
-13.8	--	14.8	--	- 47200	--	201.	0.99
- 5.47	--	7.32	--	--	610	88.2	0.78
- 0.67	--	--	-42050	515000	--	95.7	0.40
0.12	--	--	22770	--	-18480	67.2	0.49
- 0.504	--	--	--	15500	-13920	90.	0.46
--	-1.27	-0.32	-26650	--	--	172.	0.61
--	-4.99	-2.77	--	-161000	--	477	0.90
--	-0.65	1.08	--	--	- 3700	94.3	0.59
--	-4.12	--	33880	-156400	--	350.4	0.87
--	-1.62	--	-40490	--	8556	189	0.62
--	-3.45	--	--	-102000	5330	312	0.81
--	--	2.91	15570	9320	--	2.9	0.49
--	--	1.98	26490	--	-10670	27.4	0.55
--	--	1.46	--	21540	- 4720	42.3	0.50
--	--	--	88690	- 60530	-39340	64.8	0.52

* Lengths in units of nanometers, nm

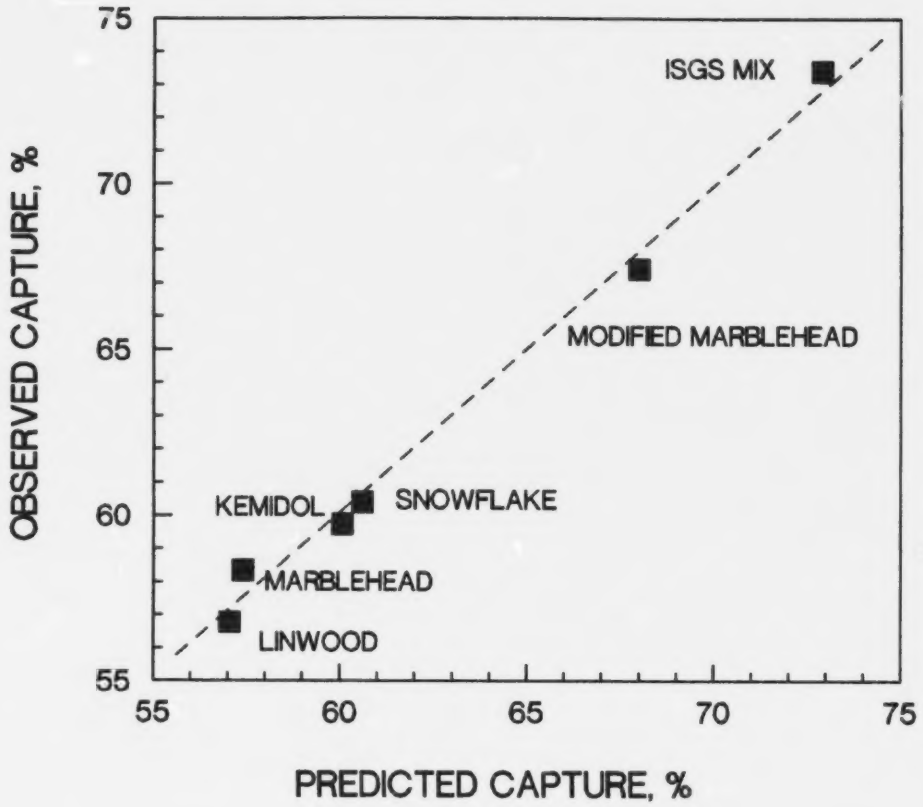

Figure B–1. Reactivity Predicted by XLB versus IFR.

All of the foregoing regressions were derived using the average reactivities for coals 1, 6, and 9. Since the average reactivities were used, the question arises as to what results would be obtained if the same regression function were used to estimate the reactivities of individual coals. The correlation coefficients for the individual coals are given in Table B-5. The LCCs for coals 1, 6, and 9 for the two best triplets of XLB factors were very good: while those of coal 2 did not indicate any significant relation at 0.19 and 0.33. Of course, coal 2 was a high pyrite coal and therefore had a different range of reactivities, making it impossible to fit.

CONCLUSIONS

The testing of sorbent materials with pilot scale and even bench scale facilities is quite resource intensive. A reliable laboratory method is needed to evaluate the numerous sources and treatments for calcium hydroxide sorbents so they can be optimized. Even after the best sorbents have been characterized, it will still be necessary to utilize the method for quality control. An effective testing method should be capable of ranking candidate sorbents in a reliable reproducible manner in any properly equipped laboratory. The ranking should be independent of gas stream makeup, reactor configuration, system temperature, and other variables. The ranking should be based on the microstructural properties of the material alone. The described technique involves the determination of reactivity from the regression of the samples' three XLB factors over a range of experimentally observed reactivities. The XLB factors of average column length, maximum column

TABLE B-5. REACTIVITY PREDICTION FROM THE TWO BEST XLB REGRESSION FUNCTIONS DERIVED FROM THE OBSERVED REACTIVITIES OF COALS #1, #6, and #9 APPLIED TO THE INDIVIDUALS COALS

IBCSP Coal	Correlation Coefficient: Average Column Length Modal Column Length Maximum Column Length	Correlation Coefficient: Average Column Length Modal Column Length Strain Modal Column Length
1	0.86	0.89
2	0.19	0.33
6	0.82	0.72
9	0.63	0.68
Average #1, #6, #9	0.96	0.99

length, and strain at the modal column length, appear to be the best estimators of reactivity from the number of samples analyzed so far. The linear correlation coefficient of 0.99 for the relation is very strong.

Even though the relation between reactivity and the three factors has been established, further work is needed. First, it is difficult to gain access to samples which have well documented reactivity. Every opportunity should be taken to run further XLB studies as more sample sorbent sets are tested for reactivity. The availability of more samples could show another triplet of XLB factors to be better. The processing of more samples, in any case, can further establish the reliability of the method. More data could also lead to the development of theory to explain the true physical meaning of the column length and mean squared strain. A new method for the interpretation of the Warren-Averbach mean squared strains has been proposed by Turunen et al. (9). The application of this theory to our data could lead to a better understanding of reactivity enhancement.

This is a new technique for the evaluation of the reactivity of solids for gases. It should be applicable wherever it is needed to optimize the reaction between solids and gases.

REFERENCES

1. Briden, F.E., and D.F. Natschke. 1989. "The Characterization of a Solid Sorbent with Crystallite Size and Strain Data from X-ray Diffraction Line Broadening." Accepted for publication in Advances in X-ray Analysis, 32.

2. Scherrer, P. 1918. "Bestimmung der Grösse und der Inneren Struktur von Kolloidteilchen Mittels Röntgenstrahlen." Nachr. Göttinger Gesell. 2, 98.

3. Schoening, F.R.L. 1965. "Strain and Particle Size Values from X-ray Line Breadths." Acta Crystallographica. 18 (5), 975.

4. Warren, B.E., and B.L. Averbach, 1950. "The Effect of Cold Work Distortion on X-ray Patterns." J. Appl. Phys. 21, 595.

5. Warren, B.E. 1969. X-ray Diffraction. Addison Wesley, Reading, MA.

6. Klug, H.P., and L.R. Alexander. 1974. X-ray Diffraction Procedures for Polycrystalline and Amorphous Materials, 2nd ed. Wiley, New York.

7. Zorn, G. "Pitfalls in the Evaluation of Diffraction Line Shape." Private communication, submitted for publication. Siemens, A.G., Corporate Research and Development, Munich, FRG, October 1987.

8. Langford, J.I., and R. Delhez. "Profile Analysis for Microcrystalline Properties by the Fourier and Other Methods." Private communication, submitted for publication. Department of Physics, University of Birmingham, Birmingham, UK, October 1987.

9. Turunen, M.J., T.H. Dekeijsen, R. Delhez, and N.M. Van der Pers. 1983. "A Method for the Interpretation of the Warren-Averbach Mean-Squared Strains and Its Application to Recovery in Aluminum." J. Appl. Cryst. 16, 172.

APPENDIX C

QUALITY CONTROL EVALUATION REPORT

QUALITY CONTROL EVALUATION REPORT

This research was sponsored by the Illinois Center for Research on Sulfur in Coal (CRSC) and did not formally require adherence to Quality Assurance guidelines as established by the Air and Energy Engineering Research Laboratory. Nonetheless, measurement activities were conducted as if the research fell under Category III project requirements. These procedures for instrument operation and quality control checks are detailed in the Quality Assurance Project Plan: LIMB Support Laboratory, prepared under EPA Contract No. 68-02-4701 by Acurex Corporation, dated May 2, 1988, and the Quality Assurance Project Plan: Limestone Injection Multistage Burner Furnace, prepared under EPA Contract No. 68-02-3988, dated May 5, 1985.

Discussion of Data Quality

The data quality will be discussed below for each measurement activity in terms of precision, accuracy, completeness, representativeness, comparative value, and corrective action. The data quality objectives for the major laboratory measurements are included in Table C-1. Four criteria were used to validate data integrity: 1) acceptable performance during calibration and accuracy tests; 2) internal consistency among observations when plotted graphically against time for a given set of conditions; 3) consistency with prior data; and 4) agreement among results obtained through independent analytical methods.

Values included in Table C-1 were calculated in the following manner:

$$\text{Accuracy} = \frac{\text{mean measured value - known value}}{\text{known value}} \times 100$$

with the exception of the Innovative Furnace Reactor (IFR) coal and sorbent feed rates where the desired value is substituted for the known value:

$$\text{Precision} = \frac{\text{standard deviation of the mean}}{\text{mean measurement}} \times 100$$

$$\text{Completeness} = \frac{\text{amount of valid data}}{\text{amount of total data}} \times 100$$

Since the SO_2 concentration is a continuous measurement, completeness has no meaning as a data quality indicator for this parameter.

The IFR coal and sorbent feeders were calibrated over the operational range prior to starting testing, then checked at the desired setting before and after each run. Checks were performed by measuring the weight of sample fed into a tared beaker as a function of time.

The SO_2 monitor was calibrated over the range of operation using three certified gases of known SO_2 concentration and a zero gas prior to the start of testing. The instrument was zeroed and spanned daily before and after testing, with the drift of the span indicated in the table.

Table C-1 Data Quality Objectives

	Accuracy		Precision		Completeness	
	Goal (%)	Achieved (%)	Goal (%)	Achieved (%)	Goal (%)	Achieved (%)
Coal feed rate (screw rate)	±10	8.2	±10	1.0	90	100
Sorbent feed rate (screw feeder)	±10	1.4	±10	6.5	90	86
SO_2 concentration (ultraviolet)	±10	5.0	±10	5.0	NA*	NA
Sulfur (ion chromatography)	± 5	2.7	± 5	1.5	90	100
Calcium (atomic absorption spectroscopy)	± 5	3.5	± 5	2.5	90	100
Particle size (x-ray sedimentation)	±10	9.5	± 8	1.4	90	100
Surface area (N_2 adsorption)	±10	2.3	±10	5.4	95	100

* NA = Not applicable

Sulfur was measured as sulfate on the ion chromatograph calibrated with three standard solutions made from a commercially available stock (Fisher Scientific). A spiked sample made independently from analytical grade Na_2SO_4 was run daily to monitor data quality along with daily laboratory blanks. Data quality for calcium determinations by atomic absorption spectroscopy was calculated in the same manner using a calcium stock solution (Fisher Scientific) and spikes made from analytical grade calcium carbonate.

Quality control checks on the x-ray sedigraph were done by running a reference garnet sample with an independently determined mean particle diameter of 2.4 μm supplied by Micromeritics. Surface area quality control checks were performed using a sample from Duke Scientific with a known surface area of 24.3 m^2/g.

All goals for data quality were met with the exception of completeness for the IFR sorbent feed. Problems with clogging of the injection probe necessitated the repeat of four tests.

Limitations on the Use of the Data

Due to inherent variability in reactor systems' time/temperature regimes, removal percentages reported in this work should not be considered as predictive of actual performance in full scale applications. The data should be considered as indicative of probable performance trends on the full scale. Likewise, values stated for coal or sorbent specific parameters (surface area, sulfur, or calcium weight percent) are not to be considered as representative of all materials produced by the respective manufacturers, but of the individual batches used in this work.

Significant QA/QC Problems

As detailed in an earlier section, plugging of the IFR sorbent injection probe led to rejection of data from four tests and necessitated their being repeated. The sorbent injection probe is currently being redesigned to enlarge the inner diameter, making clogging less likely. Procurement of a new sorbent feeder to improve data precision is also underway. As suggested by earlier researchers, the furnace was deslagged on alternating days by operation of a mid-furnace combustion lance. However, no effect on data was seen as a result of such action.